The Excitation Spectrum of a Bose-Einstein Condensate

J. Steinhauer, R. Ozeri, N. Katz, and N. Davidson
Department of Physics of Complex Systems,
Weizmann Institute of Science, Rehovot 76100, Israel

We report the first measurement of the excitation spectrum and the static structure factor of a Bose-Einstein condensate. The excitation spectrum displays a linear phonon regime, as well as a parabolic single-particle regime. The linear regime provides an upper limit for the superfluid critical velocity, by the Landau criterion. The excitation spectrum agrees well with the Bogoliubov spectrum, in the local density approximation. This agreement continues even for excitations close to the long-wavelength limit of the region of applicability of the approximation. Feynman's relation between the excitation spectrum and the static structure factor is verified, within an overall constant.

The excitation spectrum of superfluid ^{4}He gives important insights into this superfluid *[1]*. The excitation spectrum places an upper bound on the superfluid critical velocity. Furthermore, it indicates the types of excitations which occur in the superfluid, and reflects the superfluid's density correlations. The excitation spectrum of a Bose-Einstein condensate should give similar insight into this system.

The excitation spectrum is the relation $\omega(k)$, giving the energy $\hbar\omega(k)$ of each excitation, as a function of its wave vector k. For excitations with wavelengths $2\pi/k$ which are comparable to the radius of the condensate, the spectrum is characterized by discrete oscillatory modes, which are strongly dependent on the shape of the condensate. These modes have been measured previously *[2]*, *[3]*. For wavelengths much shorter than the radius of the condensate in the direction of $\vec{k}$, the excitation spectrum becomes an essentially continuous function of k, which characterizes the intrinsic bulk properties of the condensate *[4]*. In this work, "excitation spectrum" refers to this bulk regime. We report the first measurement of the excitation spectrum.

Previously, for condensates with various values of the chemical potential μ, isolated points on the excitation spectrum were measured *[5]*, *[6]*, *[7]*, *[8]*. These points, and their dependence on μ, were found to be consistent with Bogoliubov theory.

For a homogeneous condensate (constant density n), the zero-temperature excitation spectrum is expected to be of the Bogoliubov form *[9]*, which is valid as long as the wavelength of the excitation is much greater than the s-wave scattering length a. The Bogoliubov excitation spectrum is given by

$$\omega(k) = \sqrt{c^2k^2 + \left(\frac{\hbar k^2}{2m}\right)^2} \tag{1}$$

The speed of sound c is given by $\sqrt{gn/m}$, where the constant g is given by $4\pi\hbar^2 a/m$ and m is the atomic mass. The chemical potential $\mu = gn$ characterizes the strength of the atomic interactions. In the limit of small k, $\omega(k) \approx ck$. This linear part of the excitation spectrum corresponds to phonons.

By definition, $\omega(k)$ is the average frequency of the dynamic structure factor *[1]* $S(k,\omega)$, which gives the response of the excitation process. Integrating $S(k,\omega)$ over ω gives the static structure factor $S(k)$, which is the Fourier transform of the density correlation function, giving the magnitude of the density fluctuations *[10]* in the fluid, at wavelength $2\pi/k$. In general, the f-sum rule *[1]* yields Feynman's relation *[11]*

$$S(k) = (\hbar k^2/2m)/\omega(k) \tag{2}$$

Eq. 2 relates the strength of the resonance to its frequency.

For a BEC in a parabolic trap, the density is inhomogeneous, so (1) does not precisely apply. However, we will see that the form of $\omega(k)$ is very close to that of (1). In the local density approximation *[6]* (LDA), the speed of sound, and therefore the excitation spectrum (1), can be considered to be defined at each point $\vec{r}$ in the BEC, where $c = \sqrt{gn(\vec{r})/m}$. This approximation is valid as long as the Thomas-Fermi radius of the condensate in the $\vec{k}$-direction is much larger than the wavelength of the excitation *[4]*, *[6]*, *[12]*, *[13]*. For the parabolic density profile of the condensate in the Thomas-Fermi regime, the excitation spectrum for the entire condensate in the LDA is

$$\omega(k) = \sqrt{c_{ld}^2(k)k^2 + \left(\frac{\hbar k^2}{2m}\right)^2} \tag{3}$$

where $c_{ld}(k)$ is given by $\frac{\hbar k}{2m}\sqrt{S(k)^{-2}-1}$, and *[6]*, *[4]*

$$S(k) = \frac{15}{4}\left\{\frac{3+\alpha}{4\alpha^2} - \frac{3+2\alpha-\alpha^2}{16\alpha^{5/2}}\left[\pi + 2\arctan\left(\frac{\alpha-1}{2\sqrt{\alpha}}\right)\right]\right\} \tag{4}$$

where $\alpha \equiv 2\mu/[\hbar^2k^2/(2m)]$ and $\mu = gn(0)$, where $n(0)$ is the maximum density in the condensate. The value $c_{ld}\,(k)$ is a weak, monotonically increasing function, which varies from $c_{eff} \equiv 32/(15\pi)\sqrt{\mu/m}(= 0.68\sqrt{\mu/m})$ for small k, to $c_{large} = \sqrt{4/7}\sqrt{\mu/m}(= 0.76\sqrt{\mu/m})$ for large k. The value c_{large} is just the speed of sound for a homogeneous condensate whose density is the density of the inhomogeneous condensate, averaged over each atom.

Since $c_{ld}(k)$ is nearly constant, the excitation spectrum in the LDA (3) is very similar in form to the homogeneous excitation spectrum (1), illustrating that the excitation spectrum of the trapped condensate should largely reflect the intrinsic properties of the homogeneous condensate. Thus, the functional form of $\omega(k)$ reported here provides a test for the Bogoliubov theory for a homogeneous condensate.

Since small k corresponds to phonons, c_{eff} is the effective speed of sound for an inhomogeneous condensate. The Bogoliubov spectrum in the LDA fulfills the requirement of Bose statistics that the lowest lying excitations be phonons *[14]*. Phonons are collective excitations, each of which consists of a large number *[15]* N_k of atoms moving with momentum $\hbar k$, and $N_k - 1$ atoms moving with momentum -$\hbar k$. This momentum distribution of a phonon was measured in *[8]*. Previously, a sound pulse, composed of a combination of phonons, was imaged in a time sequence of absorption images *[16]*. The observed sound velocity was in rough agreement with c_{eff}.

For large k, (3) is given by

$$\omega(k) \approx \hbar k^2/(2m) + mc_{large}^2/\hbar \qquad (5)$$

where the first term is much larger than the second. This parabolic part of the spectrum corresponds to single-particle excitations, in which a single atom has a velocity $\hbar k/m$, which is much larger than the speed of sound. The second term in (5) is equal to $(4/7)\mu/\hbar$ and is independent of k, reflecting the extra interaction energy *[5]* experienced by a moving atom *[17]*.

The transition from collective excitations to single-particle excitations occurs for k on the order of ξ^{-1}, where ξ is the healing length *[18]*. We take ξ^{-1} to be the solution of $k = \sqrt{2}mc_{ld}(k)/\hbar$, which is given by $\xi^{-1} = \sqrt{2}m\overline{c}/\hbar$, and $\overline{c} \approx (c_{eff} + c_{large})/2$.

An upper limit on the superfluid critical velocity can be extracted from the excitation spectrum, via the Landau criterion, which states that the superfluid cannot flow with a speed greater than ω/k, for any excitation $\omega(k)$ in the spectrum *[1]*. Therefore, the critical velocity v_c cannot be more than the smallest value of ω/k in the entire spectrum. According to Bogoliubov theory, the phonons have the smallest value of ω/k, as seen in Fig. 2a, so v_c cannot be greater than the speed of sound c_{eff}. We emphasize that the critical velocity for vortex production is usually much lower than the critical velocity given by the Landau criterion, so vortex production usually limits the speed of superfluid flow *[19]*, *[20]*.

The condensate of ^{87}Rb atoms in the $5s_{1/2}$, $F = 2$, $m_F = 2$ ground state is produced in a QUIC magnetic trap *[21]*, loaded by a double MOT system. The magnetic trap contains $6{\times}10^7$ atoms. After 22 seconds of evaporation, $1{\times}10^5$ atoms remain, forming a nearly pure condensate, with a thermal fraction of 5% or less. The bias magnetic field is 2 G. The radial and axial trapping frequencies are 25 Hz and 220 Hz respectively, yielding radial and axial Thomas-Fermi radii of 3 μm and $R = 28$ μm, respectively. The chemical potential $\mu/h = 2.02 \pm 0.09$ kHz is determined *[22]* by the radial size of the condensate in a time-of-flight image.

The excitation spectrum is measured by Bragg spectroscopy *[5]*, *[23]*. Two Bragg beams A and B with approximately parallel polarization *[24]*, separated by an angle $3^o \leq \theta \leq 130^o$, illuminate the condensate for a time t_B. The frequency of beam A is greater than the frequency of beam B by an amount ω determined by two acousto-optic modulators. If a photon is absorbed from A and emitted into B, an excitation is produced with energy ω and momentum k, where $k = 2k_p \sin(\theta/2)$, and k_p is the photon wave number. Here, we neglect the possibility that a single photon will excite multiple excitations, in contrast to the case of superfluid ^{4}He, in which multiparticle excitations are an important contribution *[25]*, *[1]* to $S(k, \omega)$.

The wave vector $\overrightarrow{k}$ is precisely adjusted to be along the axis of the cigar-shaped condensate *[26]*. To insure that the entire condensate is stimulated by the Bragg pulse, the length of the pulse t_B is chosen such that the spectral width of the pulse is roughly equal to the intrinsic width of the resonance. For this experiment, the broadening due to inhomogeneous density $\Delta\nu_{ld}$ always dominates the Doppler broadening *[5]*, and is given by *[4]* 0.45 kHz for large k, and 0.3 $\omega(k)/(2\pi)$ in the phonon regime. Thus, t_B is chosen to be roughly $(2\Delta\nu_{ld})^{-1}$. For large k, the resonance may be further broadened by s-wave scattering *[27]*.

The beams are detuned $\Delta = 6.5$ GHz below the $5S_{1/2}$, $F = 2 \rightarrow 5P_{3/2}$, $F = 3$ transition. The intensities I_A and I_B of each beam are adjusted to values between 0.1 mW cm^{-2} and 1.1 mW cm^{-2} *[28]*, so that the number of excitations is 10% to 20% of the number of atoms in the condensate. For pulses of this strength, the chemical potential decreases by an average of only 12% during the pulse, so the Bragg scattering can be considered to be a small perturbation to the condensate. The time average of μ/h during the pulse is 1.91 ± 0.09 kHz, which is taken to be the relevant value for the excitation spectrum.

To measure a single point on the excitation spectrum $\omega(k)$, k is fixed by θ, and ω is varied. The resonant value of ω is taken as $\omega(k)$.

After the Bragg pulse, the atoms are allowed to expand freely, after which they are imaged by absorption *[29]*, as shown in Fig. 1 for k within the phonon regime. Two adjacent clouds are seen. The left cloud corresponds to the condensate. The right cloud, displaced in velocity space by $\hbar k/m$, corresponds to the excitations. During the time-of-flight, the density of the atomic cloud decreases dramatically, resulting in a decrease in the speed of sound. The phonons of wave number k are thus transformed *[6]* into free particles, which are subsequently im-

FIG. 1. The Bragg and condensate clouds. (a) Average of 2 absorption images after 38 msec time-of-flight, following a resonant Bragg pulse with $k = 2.8\ \mu m^{-1}$, in the phonon regime. (b) Cross-section of the same image. The dashed line is a Gaussian fit to the condensate cloud, used to find the zero of momentum. The radial and axial coordinates are indicated by r and z, respectively.

To determine the efficiency of stimulation of excitations by the Bragg pulse, the total momentum in the axial direction relative to the center of the condensate cloud is computed from the image, in the combined regions of the two clouds *[30]*. The total momentum is divided by $N_o\hbar k$, where N_o is the average number of atoms in the condensate during the Bragg pulse, to obtain the efficiency. This efficiency is somewhat exaggerated though, because the total momentum includes momentum from the release process.

The thus-measured efficiency $P(k,\omega)$ for each direction is shown in Fig. 2, for $k = 2.8\ \mu m^{-1}$. The curve of $P(k,\omega)$ is well-approximated by a Gaussian plus a constant. The constant results from the background in the images. The symmetric shape of $P(k,\omega)$ about the resonance frequency probably reflects the spectral shape of the Bragg pulse, rather than the intrinsic shape which is expected to be asymmetric *[4]*. Therefore, the notation $P(k,\omega)$ is employed, rather than $S(k,\omega)$, whose shape is the intrinsic shape.

The resonant frequency is taken as the center value of the Gaussian fit to $P(k,\omega)$, as shown in Fig. 2. The excitation energy $\omega(k)$ is taken as the average of the resonant frequencies for the left and right directions, which removes the effects of the Doppler shift resulting from any sloshing of the condensate in the trap during the Bragg pulse.

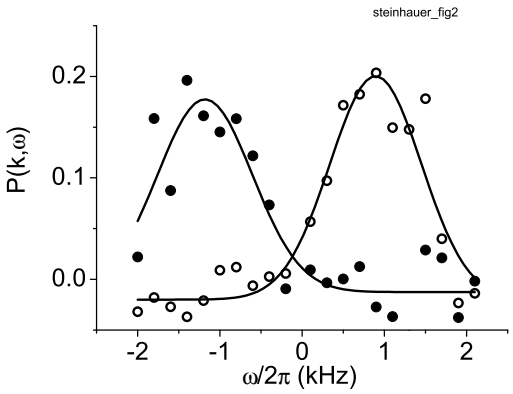

FIG. 2. The efficiency $P(k,\omega)$ for $k = 2.8\ \mu m^{-1}$. The open and filled circles are for left and right-travelling clouds, respectively. The lines are fits of a Gaussian plus a constant.

The integral of $P(k,\omega)$ over ω, equal to the integral of $S(k,\omega)$, is related to $S(k)$ by [31]

$$S(k) = 2(\pi\Omega_R^2 N_o t_B)^{-1} \int P(k,\omega) d\omega \qquad (6)$$

where $\Omega_R = \Gamma^2/(4\Delta)\sqrt{I_A I_B}/I_{sat}$ is the two-photon Rabi frequency, Γ is the line width of the $5P_{3/2}$, $F = 3$ excited state, and I_{sat} is the saturation intensity.

Fig. 3a shows the measured excitation spectrum. The solid line is the Bogoliubov spectrum in the LDA (3), without any fit parameters, for $\mu = 1.91$ kHz. The measured spectrum is seen to agree well with the Bogoliubov spectrum. A linear phonon regime is seen for low k, and a parabolic single-particle regime for high k. The line at $k = \xi^{-1}$ separates these two regimes. The excitations seen to have the smallest value of ω/k are the phonons. Therefore, by the Landau criterion, the superfluid velocity v_c is bounded by ω/k for the phonons.

The inset of Fig. 3a shows the low k region of the excitation spectrum. To extract the initial slope from the data, (3) is fit to the points with k less than 3 μm^{-1}, with μ taken as a fit parameter. The fit is not shown in the figure. The result gives the speed of sound for the condensate to be $c_{eff} = 2.0 \pm 0.1$ mm sec^{-1}, which is also the measured upper bound for v_c, by the Landau criterion. This value is in good agreement with the theoretical value of 2.01 ± 0.05 mm sec^{-1}, which is the $k = 0$ slope of the Bogoliubov spectrum for $\mu = 1.91 \pm 0.09$ kHz. The line at $2\pi R^{-1}$ indicates the excitation whose wavelength is equal to the Thomas-Fermi radius of the

condensate in the axial direction. The measured excitation spectrum agrees with the LDA, even for k values approaching this lower limit of the region of validity. For the two lowest k-values measured, the wavelength of the excitations are long enough that they are clearly visible, as density modulations in the condensate cloud.

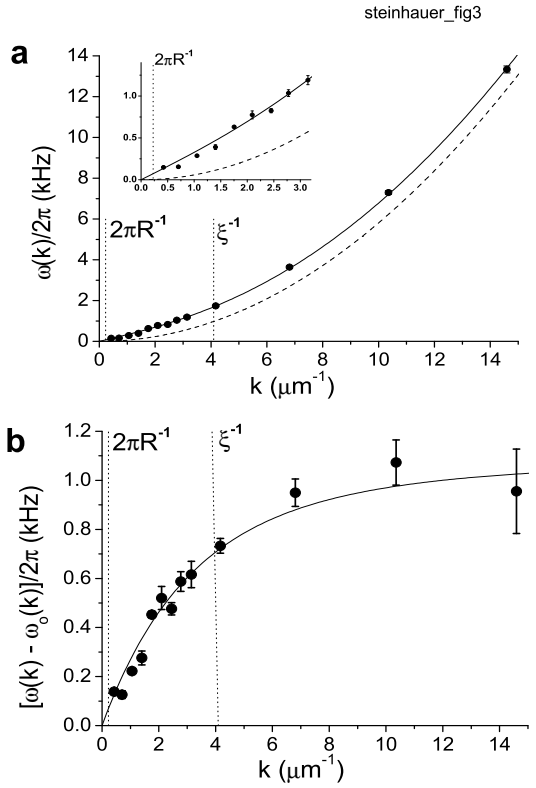

FIG. 3. (a) The measured excitation spectrum $\omega(k)$ of a trapped Bose-Einstein condensate. The solid line is the Bogoliubov spectrum with no free parameters, in the LDA for $\mu = 1.91$kHz. The dashed line is the parabolic free-particle spectrum. The vertical line at ξ^{-1} shows the separation between the collective and single-particle regimes. The vertical line at $2\pi R^{-1}$ shows the lower limit of the region of validity of the LDA. For most points, the error bars are not visible on the scale of the figure. The inset shows the linear phonon regime. (b) The difference between the excitation spectrum and the free-particle spectrum. Error bars represent 1σ statistical uncertainty. The theoretical curve is the Bogoliubov spectrum in the LDA for $\mu = 1.91$ kHz, minus the free-particle spectrum.

Fig. 3a also shows the parabolic spectrum for free particles, $\hbar k^2/(2m)$. The measured excitation spectrum is clearly above this curve, reflecting the interaction energy of the condensate. To emphasize the interaction energy, $\omega(k)$ is shown again in Fig. 3b, after subtraction of the free-particle spectrum. The theoretical curve is the Bogoliubov spectrum in the LDA, given by (3), minus the parabolic spectrum for free atoms. This curve approaches a constant for large k, given by the second term in (5).

The closed circles in Fig. 4 are the measured static structure factor $S(k)$, by (6). The values shown have been increased by a factor of 2.3, giving rough agreement with $S(k)$ from Bogoliubov theory in the LDA (4). Eq. (4) is indicated by a solid line. The required factor of 2.3 probably reflects inaccuracies in the various values needed to compute Ω_R. The open circles are computed from (2), using the measured values of $\omega(k)$ shown in Fig. 3a. The rough agreement between the closed and open circles is consistent with the relation (2), within the multiplicative constant applied to the closed circles. For the determination of $S(k)$, it is critical that the apparent number of excitations is not enhanced by extra momentum obtained during the release process. Therefore, the number of excitations is determined by the number of atoms in the excitation cloud, rather than by the total momentum. This technique fails for the two points with the lowest k values, where many of the atoms do not exit the condensate cloud. For these points, the measured $S(k)$ seen in Fig. 4 is significantly reduced.

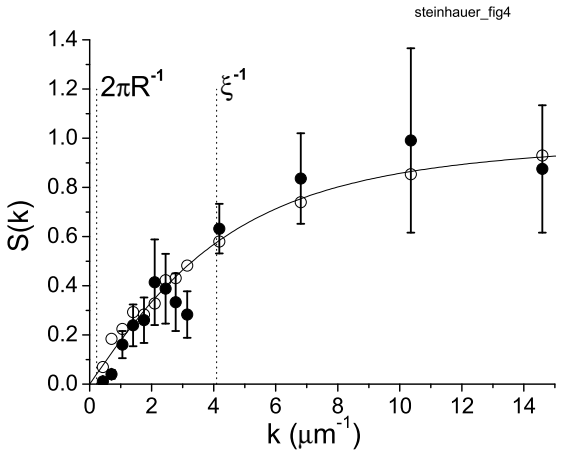

FIG. 4. The filled circles are the measured static structure factor, multiplied by an overall constant of 2.3. Error bars represent 1σ statistical uncertainty, as well as the estimated uncertainty in the two-photon Rabi frequency. The solid line is the Bogoliubov structure factor, in the LDA for $\mu = 1.91$ kHz. The open circles are computed from the measured excitation spectrum of Fig. 3, and Feynman's relation (2). For the open circles, the error bars are not visible on the scale of the figure.

For large k (short wavelength), $S(k)$ approaches unity, corresponding to non-interacting, uncorrelated atoms. For long wavelengths however, $S(k)$ counterintuitively approaches zero. For decreasing k, the condensate

contains increasing numbers of atoms with momentum $\hbar k$. These atoms, rather than creating additional density fluctuations with wavelength $2\pi/k$, actually suppress such fluctuations, because the atoms are correlated in pairs with momenta $\pm\hbar k$, and opposite phase *[6]*.

Since $S(k)$ is always less than unity for the values of k measured here, the density fluctuations are never greater than in the uncorrelated case. However, $S(k)$ is expected to have a peak (a roton) at a wavelength comparable to a, which is much shorter than the wavelengths reported here, but the increase of $S(k)$ at this roton is on the order of a^3n. For a BEC in an alkali gas, $a^3n \sim 10^{-4}$, so the roton is negligible. This is in contrast to superfluid ^{4}He, where $S(k)$ has a significant roton, corresponding to a minimum in $\omega(k)$.

For $k \geq 6.8\ \mu m^{-1}$, s-wave scattering is clearly visible. The measured effective scattering cross section decreases with decreasing k, as predicted in *[32]*.

In conclusion, we report the first measurement of the excitation spectrum of a Bose-Einstein condensate, and the static structure factor. This spectrum displays several features consistent with theory. The excitation spectrum consists of a linear phonon regime, as well as a single-particle regime. The linear regime provides an upper limit for the superfluid critical velocity, by the Landau criterion. The excitation spectrum agrees quantitatively with the Bogoliubov spectrum, in the local density approximation. This agreement continues even for long-wavelength excitations, close to the limit of the region of applicability of the approximation. The density fluctuations implied by the static structure factor agree with the excitation spectrum within a multiplicative constant, via Feynman's relation. Feynman's relation is thus verified within an overall constant.

[1] Ph. Nozieres and D. Pines, *The Theory of Quantum Liquids* (Addison-Wesley, 1990), Vol. II.
[2] D. S. Jin, et al., Phys. Rev. Lett. **77**, 420 (1996).
[3] M. O. Mewes et al, Phys. Rev. Lett. **77**, 988 (1996).
[4] F. Zambelli, et al, Phys. Rev. A **61**, 063608 (2000).
[5] J. Stenger et al, Phys. Rev. Lett. **82**, 4569 (1999).
[6] D. M. Stamper-Kurn et al., Phys. Rev. Lett. **83**, 2876 (1999).
[7] S. Inouye et al., Phys. Rev. Lett. **85**, 4225 (2000).
[8] J. M. Vogels et al., cond-mat 0109205.
[9] N. N. Bogoliubov, J. Phys. (USSR) **11**, 23 (1947).
[10] D. Pines and Ph. Nozieres, *The Theory of Quantum Liquids* (Addison-Wesley, 1966, 1988), Vol. I.
[11] This relation is derived by other means in R. P. Feynman, Phys. Rev. **94**, 262 (1954).
[12] In E. Zaremba, Phys. Rev. A **57**, 518 (1998), and in [13], the speed of sound for axial propagation in a cigar shaped condensate is shown to be approximately the LDA value, even for wavelengths larger than the transverse size of the condensate.
[13] S. Stringari, Phys. Rev. A **58**, 2385 (1998).
[14] K. Huang, *Statistical Mechanics* (Wiley, New York, 1987).
[15] A. Brunello, et al, Phys. Rev. Lett. **85**, 4422 (2000).
[16] M.R. Andrews, et al, Phys. Rev. Lett. **79**, 553 (1997) and Erratum, Phys. Rev. Lett. **80**, 2967 (1998).
[17] A. J. Leggett, Rev. Mod. Phys. **73**, 307 (2001).
[18] G. Baym and C. J. Pethick, Phys. Rev. Lett. **76**, 6 (1996).
[19] C. Raman, et al, Phys. Rev. Lett. **83**, 2502 (1999).
[20] R. J. Donnelly, *Quantized Vortices in HeII* (Cambridge University Press, New York, 1991).
[21] T. Esslinger et al., Phys. Rev. A **58**, R2664 (1998).
[22] Y. Castin and R. Dum, Phys. Rev. Lett. **77**, 5315 (1996).
[23] M. Kozuma et al, Phys. Rev. Lett. **82**, 871 (1999).
[24] Although the polarization is not along the axis of the condensate, superradiance has not been observed in this system. See S. Inouye et al., Science **285**, 571 (1999).
[25] A. Griffin, *Excitations in a Bose-Condensed Liquid* (Cambridge University Press, Cambridge, England, 1993).
[26] For two points on the excitation spectrum, k is not along the axis of the condensate. Specifically, for $k = 14.6\ \mu m^{-1}$ and $k = 4.2\ \mu m^{-1}$, $\overrightarrow{k}$ is 25° and 4° from the axis, respectively. For both of these k-values however, the wavelength is much smaller than the Thomas-Fermi radius in the direction of propagation.
[27] s-wave scattering may cause a very small shift in $\omega(k)$, which we neglect.
[28] Spontaneous scattering is negligible for these intensities.
[29] Typically, 4 images are averaged for each value of ω and k.
[30] Since the excitation cloud contains few atoms, and overlaps the condensate, it is difficult to distinguish between atoms in the excitation cloud and atoms in the thermal cloud. Therefore, the cutoff frequency of the evaporation is adjusted for each image with a precision of 2 kHz, so that the measured thermal fraction is no more than 5%.
[31] The constant rate of production of excitations is given in W. Ketterle and S. Inouye, e-print cond- mat/0101424 29.
[32] A. P. Chikkatur, et al, Phys. Rev. Lett. **85**, 483 (2000).

[33] This work was supported by the Israel Science Foundation.